

# Effects of Ligand Monolayers on Catalytic Nickel Nanoparticles for Synthesizing Vertically Aligned Carbon Nanofibers

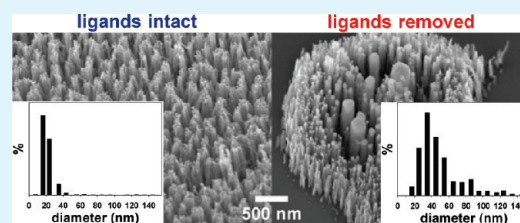
Mehmet F. Sarac,<sup>†</sup> Robert M. Wilson,<sup>†</sup> Aaron C. Johnston-Peck,<sup>†</sup> Junwei Wang,<sup>†,‡</sup> Ryan Pearce,<sup>†</sup> Kate L. Klein,<sup>§</sup> Anatoli V. Melechko,<sup>†</sup> and Joseph B. Tracy<sup>\*,†</sup>

<sup>†</sup>Department of Materials Science and Engineering, North Carolina State University, Raleigh, North Carolina 27695, United States

<sup>§</sup>Surface and Microanalysis Science Division, National Institute of Standards and Technology, 100 Bureau Drive, Gaithersburg, Maryland 20899, United States

**ABSTRACT:** Vertically aligned carbon nanofibers (VACNFs) were synthesized using ligand-stabilized Ni nanoparticle (NP) catalysts and plasma-enhanced chemical vapor deposition. Using chemically synthesized Ni NPs enables facile preparation of VACNF arrays with monodisperse diameters below the size limit of thin film lithography. During pregrowth heating, the ligands catalytically convert into graphitic shells that prevent the catalyst NPs from agglomerating and coalescing, resulting in a monodisperse VACNF size distribution. In comparison, significant agglomeration occurs when the ligands are removed before VACNF growth, giving a broad distribution of VACNF sizes. The ligand shells are also promising for patterning the NPs and synthesizing complex VACNF arrays.

**KEYWORDS:** carbon nanofibers, nanoparticles, nickel, chemical vapor deposition, catalyst, ligand



## INTRODUCTION

The synthesis of ligand-stabilized nanoparticles (NPs) has attracted intense interest because of their anticipated applications in optoelectronics,<sup>1</sup> magnetics,<sup>2</sup> catalysis,<sup>3</sup> and biomedicine.<sup>4</sup> Apart from the magnetic properties of the 3d-ferromagnets, Fe, Co, and Ni are also well-known as catalysts for growing carbon nanostructures.<sup>5–8</sup> There is strong interest in improving control over the uniformity and patterning of carbon nanotubes (CNTs), carbon nanofibers (CNFs), and inorganic nanowires by controlling the composition, size,<sup>8</sup> and assembly of the catalyst NPs. Synthesizing CNFs with uniform diameters requires both a uniform catalyst NP size distribution and thermal stability up to temperatures of 700 °C, at which CNF growth is initiated. In the synthesis of vertically aligned carbon nanofibers (VACNFs) by plasma-enhanced chemical vapor deposition (PECVD), the nanofibers grow from catalyst NPs that have been deposited or patterned on a substrate.<sup>9</sup> When using Ni NP catalysts, as reported here, VACNFs are known to grow through tip-type growth, where the catalyst NP is attached to the free end of the CNF.<sup>9</sup> Agglomeration is no longer possible once the catalyst NPs have been lifted above the substrate at the beginning of CNF growth. VACNFs have been used as electron field emitters,<sup>10</sup> tips for atomic force microscopy,<sup>11</sup> elements of solar cells,<sup>12</sup> intracellular electrodes,<sup>13</sup> and as porous membranes for biomimetic cells.<sup>14</sup> Obtaining uniform and controllable VACNF size distributions is crucial for achieving the desired function in such applications, which generally requires that agglomeration of the catalyst NPs be avoided.

Many methods for chemically synthesizing ligand-stabilized Fe<sub>x</sub>O<sub>y</sub>,<sup>15–20</sup> Co,<sup>21–24</sup> and Ni<sup>25–29</sup> NPs with size control have been developed. The ligand shells are also potentially useful for their ability to facilitate patterning of the catalyst NPs. In comparison

to the extensively developed methods for NP synthesis,<sup>30</sup> much less is known about how to prevent NPs from agglomerating at high temperatures. Although covering metal NPs with oxide shells is known to prevent agglomeration,<sup>31</sup> significant surface coverage of catalyst NPs with inorganics would likely perturb the reaction products during carbon nanostructure growth. Encapsulating NPs with graphitic shells has also been shown to protect against agglomeration at high temperatures or under harsh chemical environments.<sup>32,33</sup>

Here, we report a study of the effects of ligands covering Ni catalyst NPs on the synthesis of VACNFs, and we show that the ligands catalytically convert into graphitic shells that prevent agglomeration at high temperatures, resulting in a monodisperse distribution of VACNF diameters that correlates with size of the Ni NPs. In samples where the ligands were removed prior to VACNF growth, significant agglomeration and coalescence occurred, which gave a broad distribution of VACNF diameters. Further benefits of ligand-stabilized NPs are their tunable sizes and facile preparation and deposition onto substrates for VACNF growth. Methods utilizing chemically prepared NPs are potentially more reproducible and less expensive than lithography and thin film dewetting approaches that are commonly employed for VACNF growth.<sup>34</sup>

## RESULTS AND DISCUSSION

Ligand-stabilized Ni NPs were synthesized by the high-temperature reduction of nickel(II) acetylacetonate in the presence of trioctylphosphine (TOP) and oleylamine (OLA)

**Received:** December 31, 2010

**Accepted:** February 28, 2011

**Published:** March 16, 2011

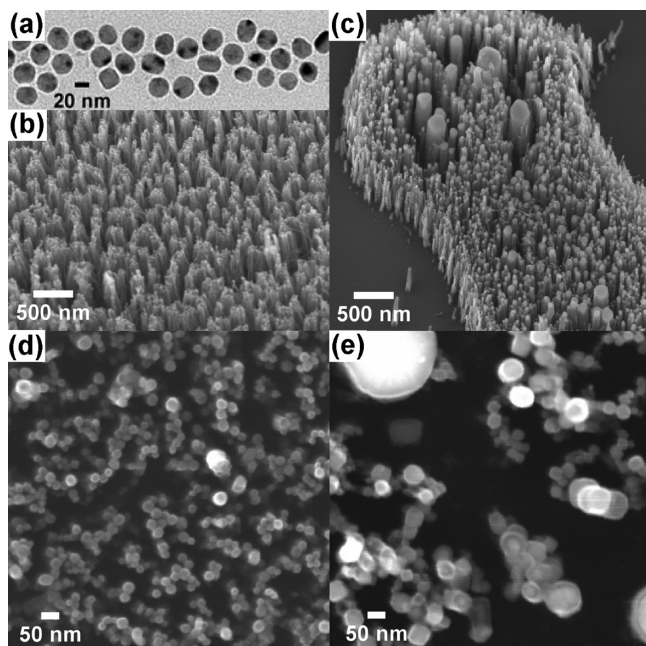


**Figure 1.** (a) TEM image of ligand-stabilized Ni NPs with an average diameter of 25 nm before VACNF growth. SEM images of (b, c) 30° tilted views and (d, e) top views of VACNFs grown from the Ni NPs (b, d) without ligand removal and (c, e) after ligand removal.

ligands.<sup>28</sup> Phosphines interact more strongly with the Ni surface than amines; after purification, the ligand monolayer coating the NPs contains only TOP. Measurements of the Ni NPs by transmission electron microscopy (TEM) show that they have spherical shapes with an average diameter of 25 nm (Figure 1a). By adjusting the reaction conditions, the diameter could be tuned between 8 and 100 nm.<sup>28,29</sup> Scanning electron microscopy (SEM) images of the VACNFs (Figure 1) show distinctly different diameter distributions (Figure 2), depending whether the ligands had been removed.

Leaving the ligands intact resulted in highly monodisperse sizes. The histogram of the VACNF diameters for growth from Ni NPs whose ligands were not removed shows a narrow size distribution, with a mean NP diameter of 21 nm (Figure 2a). In comparison, ligand removal from the same batch of catalyst NPs by treatment with ultraviolet light and ozone (UVO) resulted in an average diameter of 46 nm and a significantly broader size distribution (Figure 2b, where the largest sizes lie outside of the range of the histogram). Therefore, leaving the ligands intact suppressed agglomeration and resulted in diameters very close to the size of the catalyst NPs, but ligand removal caused substantial agglomeration and coalescence.

These results imply that bare NPs (after ligand removal) agglomerate and coalesce before VACNF growth begins. Agglomeration is possible only before VACNF growth starts,<sup>35</sup> because Ni NPs catalyze tip-type growth of VACNFs, which lifts the catalyst NPs off the surface of the substrate.<sup>9</sup> This pregrowth phase includes heating the substrate to 700 °C under a reducing ammonia (NH<sub>3</sub>) atmosphere followed by a brief period of plasma heating<sup>36</sup> after acetylene has been introduced, until graphitic layers start to form under the NPs. In a prior study from our group that used identical UVO treatment conditions for ligand removal, the UVO treatment at room temperature did not itself cause agglomeration.<sup>37</sup>

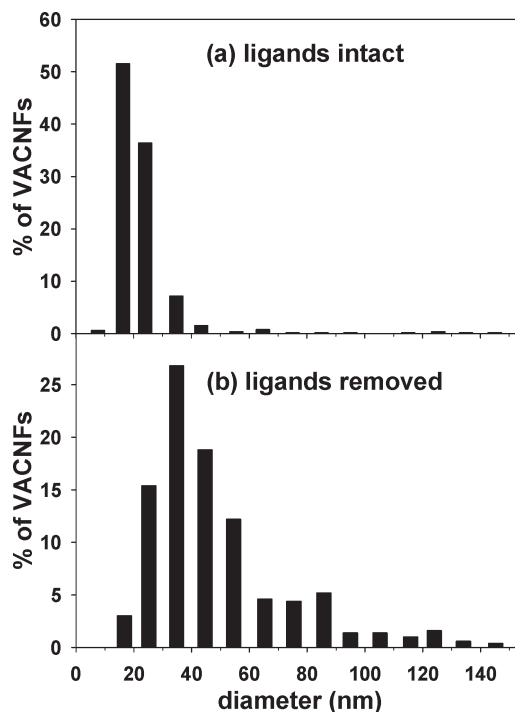


**Figure 2.** Histograms of the diameters of VACNFs grown from Ni catalysts, measured from SEM images acquired at 100 000 magnification with a measurement uncertainty of  $\pm 5$  nm for 500 nanofibers in each sample: (a) with ligands intact or (b) after ligand removal. Some VACNFs after ligand removal had diameters greater than 150 nm that are not tabulated.

Several reports of similar experiments have shown that the ligands can be converted into graphitic shells while heating in a reducing atmosphere.<sup>33,38,39</sup> A plausible mechanism for conversion into graphitic shells (Figure 3a–d) includes three main steps: (i) Nickel NPs catalytically decompose TOP at  $\approx 300$  °C,<sup>29</sup> which liberates elemental phosphorus and hydrocarbon chains. (ii) At  $\approx (400–500)$  °C, the Ni NPs catalytically decompose the hydrocarbons into atomic carbon, (iii) which is then restructured into graphitic layers.<sup>40</sup> Some of the hydrocarbons could also desorb from the NP surfaces, and some of the atomic carbon might also dissolve in the NP core. To test this hypothesis, a set of annealing experiments was performed, in which NPs with intact ligands were deposited onto thermally robust TEM substrates, followed by annealing at (450 or 700) °C under a NH<sub>3</sub> atmosphere for 10 min. The products after annealing at 700 °C are encapsulated by one or two graphitic layers (Figure 3g, h). We further note that the ligands also serve as an ample carbon source for the start of nanotube growth, when the graphitic shell detaches from one side of the NP (Figure 3g, h). The solid-state, catalytic conversion of amorphous carbon has been extensively studied by in situ TEM.<sup>41,42</sup>

The pregrowth phase is the critical process, when the ligands are converted into graphitic shells that encapsulate the NPs and protect against agglomeration by preventing transport of Ni along the surface of the substrate. In contrast, after ligand removal, the bare NPs lack a carbon source for forming graphitic shells, which allows mobility on the substrate at high temperatures that gives rise to agglomeration. In these experiments, the native oxide on the Si substrates is sufficient for eliminating interdiffusion of Ni and Si as a possibility.<sup>8</sup> Previously, depth



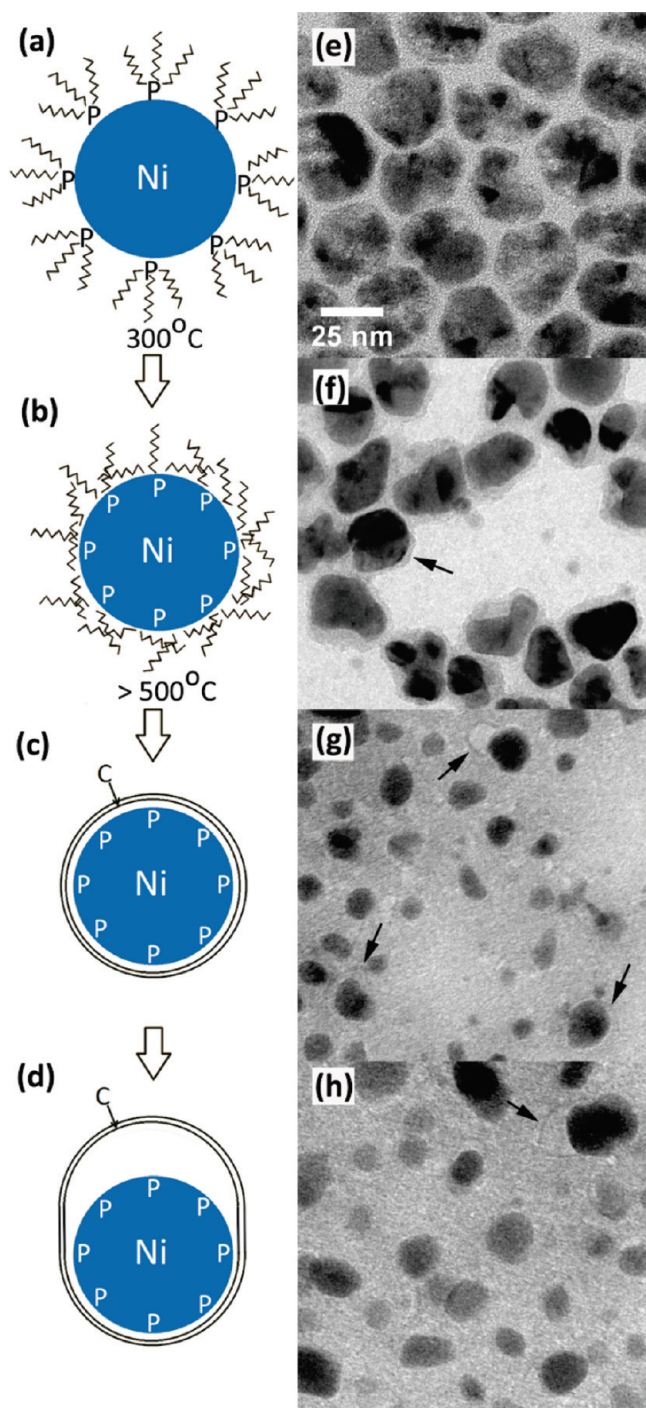


**Figure 3.** (a–d) Graphical depiction of the decomposition of triethylphosphine on a Ni NP and its conversion into a graphitic shell; bright-field TEM images (with a common scale bar) of Ni NPs with ligands intact (e) prior to heating, and after annealing for 10 min under  $\text{NH}_3$  atmosphere (f) at 450 °C (arrow indicates the shell surrounding a NP) and (g, h) at 700 °C (arrows point to a fringes of graphitic layers).

profiling with an Auger microprobe has shown that the Ni content in the substrate is undetectable.<sup>43</sup> On a time scale of several hours, however, interdiffusion and silicide formation cannot be excluded from consideration.<sup>44</sup>

Control over the catalyst NP size and eliminating agglomeration are critical factors for growing uniform sizes of VACNFs and

for fully realizing their applications, because the VACNF diameter often controls the functionality. For example, in the case of electron field emitters, the field enhancement factor is proportional to the fiber length to tip diameter ratio. In nanospearing of cells for gene delivery, the VACNF diameter determines its ability to penetrate the cell membrane.<sup>45</sup> Catalyst NPs for VACNF growth are commonly prepared by dewetting metal thin films, which produces a broad size distribution, whose average size increases with increasing film thickness.<sup>46</sup> Dewetting of thin films patterned by photolithography is useful for producing NPs with uniform diameters greater than 100 nm. Electron beam lithography (EBL) can be used to pattern smaller NPs with sizes of a few tens of nanometers.<sup>34</sup> Use of EBL adds significant complexity and cost that is especially problematic for commercialization, but this chemical synthetic approach allows facile preparation of small catalyst NPs with narrow size distributions. We anticipate that soft lithography techniques, such as micro-contact printing, could be useful for patterning chemically synthesized NPs. Moreover, the ligands on ligand-stabilized NPs prevent agglomeration and coalescence of the catalyst NPs at the high VACNF growth temperatures, giving rise to a monodisperse VACNF size distribution that is controlled by the size of the catalyst NPs.

## CONCLUSIONS

Chemical synthesis is an appealing approach for preparing catalyst NPs for VACNF growth. Synthetic methods are already well established for obtaining highly monodisperse ligand-stabilized NPs with tunable sizes. Here, we have shown that when using ligand-stabilized Ni NPs for catalyzing VACNF growth, the ligands also serve a critical role in preventing the NPs from agglomerating, which gives a monodisperse VACNF size distribution. The ligands are converted into protective graphitic shells. If the ligands are removed after deposition on the substrate, ligand removal does not itself cause agglomeration, but substantial agglomeration of bare NPs occurs during heating in the pregrowth phase, which results in larger, polydisperse VACNF sizes. We are currently investigating how to extend these results to the synthesis of complex patterns of VACNFs by patterning the ligand-stabilized catalyst NPs.

## EXPERIMENTAL SECTION<sup>47</sup>

**Nickel Nanoparticle Synthesis and Characterization.** Ni NPs with average diameters of 25 nm were synthesized following a method that we recently reported.<sup>28</sup> Amounts of 0.200 g of nickel acetylacetonate ( $\text{Ni}(\text{acac})_2$ , 98 %, TCI America), 2.0 mL of oleylamine (OLA, 97 %, Pfaltz & Bauer), and 5.0 g of triethylphosphine oxide (TOPO, 99 %, Strem) were heated at 60 °C in a three-necked, round-bottomed flask for 1.5 h under a vacuum to remove oxygen before backfilling with nitrogen. By syringe, 0.1 mL of triethylphosphine (TOP, 97 %, Strem) was injected into the mixture before rapidly heating the solution to 240 °C (over  $\approx 10$  min) with vigorous stirring. After aging for 30 min at 240 °C, the mixture was cooled to room temperature. The product was isolated from the high-boiling solvent and excess ligands by adding methanol, briefly centrifuging and then discarding the supernatant and redispersing the NPs in hexanes. The NP size was measured using a JEOL 2000FX transmission electron microscope (TEM).

**VACNF Synthesis and Characterization.** A solution of the Ni NPs with a concentration of 1 wt % in hexanes was spin-cast onto small ( $\approx 1 \text{ cm}^2$ ) Si substrates (As-doped,  $1\text{--}10 \text{ }\Omega\text{-cm}$ ), which provides approximate monolayer coverage. Ligand removal was performed on one set of samples by treatment with ultraviolet light and ozone (UVO)<sup>37,48</sup> for 4 min. The samples were loaded into the growth chamber at room temperature, followed by evacuation to 13 Pa. Flowing ammonia ( $\text{NH}_3$ ) vapor was introduced into the chamber and equilibrated at a flow rate of  $85 \text{ cm}^3/\text{min}$  and pressure of 533 Pa, which was maintained throughout the growth. While keeping the pressure constant at 533 Pa, the temperature was increased to  $(700 \pm 5) \text{ }^\circ\text{C}$ . Once the chamber reached  $700 \text{ }^\circ\text{C}$ , flowing acetylene ( $\text{C}_2\text{H}_2$ ) was switched on at rate of  $60 \text{ cm}^3/\text{min}$ . After waiting 10 s, the plasma was turned on with a current of 200 mA and ramp time of 15 s. After completing 10 min of growth, the plasma,  $\text{NH}_3$ ,  $\text{C}_2\text{H}_2$ , and the heater were turned off, and the chamber was evacuated and cooled to  $100 \text{ }^\circ\text{C}$  before venting with nitrogen and unloading the samples. Images of the VACNFs were acquired using a Hitachi S-4700 field-emission scanning electron microscope. For plotting histograms of the diameters, the diameters of 500 VACNFs were measured for each sample.

**Characterization of the PREGROWTH PROCESS.** For characterizing the evolution of the Ni NPs with ligands intact prior to growth by TEM (Figure 3), three samples were prepared. The ligand-coated Ni NPs were imaged as-deposited on  $\text{SiO}$  films (Ted Pella, product number 01829). An identical specimen was heated at  $450 \text{ }^\circ\text{C}$  under an  $\text{NH}_3$  atmosphere for 10 min on an  $\text{SiO}$  film. The third sample was deposited onto a 50 nm thick  $\text{SiN}$  membrane (Protochips, DuraSiN) and was heated to  $700 \text{ }^\circ\text{C}$  under a  $\text{NH}_3$  atmosphere for 10 min. The sample that was not annealed was imaged using a JEOL 2000FX TEM, and the annealed samples were imaged using a Philips/FEI CM300FEG TEM.

## AUTHOR INFORMATION

### Corresponding Author

\*jbracy@ncsu.edu.

### Present Addresses

<sup>†</sup>Department of Materials Science and Engineering, Rensselaer Polytechnic Institute, Troy, New York 12180, United States

## ACKNOWLEDGMENT

This work was supported by startup funds from North Carolina State University and by the National Science Foundation (CBET-0967559). A.V.M. acknowledges support from the Materials Sciences and Engineering Division, Office of Basic Energy Sciences, U.S. Department of Energy. M.F.S. acknowledges support from a Republic of Turkey, Ministry of National Education fellowship. A.C.J.-P. acknowledges support from a GAANN fellowship. We thank Protochips, Inc., for providing the  $\text{SiN}$  substrates.

## REFERENCES

- (1) Talapin, D. V.; Lee, J. S.; Kovalenko, M. V.; Shevchenko, E. V. *Chem. Rev.* **2010**, *110*, 389–458.
- (2) Lu, A. H.; Salabas, E. L.; Schüth, F. *Angew. Chem., Int. Ed.* **2007**, *46*, 1222–1244.
- (3) Aiken, J. D.; Finke, R. G. *J. Mol. Catal. A: Chem.* **1999**, *145*, 1–44.

- (4) De, M.; Ghosh, P. S.; Rotello, V. M. *Adv. Mater.* **2008**, *20*, 4225–4241.
- (5) Merkulov, V. I.; Melechko, A. V.; Guillorn, M. A.; Simpson, M. L.; Lowndes, D. H.; Whealton, J. H.; Raridon, R. J. *Appl. Phys. Lett.* **2002**, *80*, 4816–4818.
- (6) Zhong, Z. Y.; Chen, H. Y.; Tang, S. B.; Ding, J.; Lin, J. Y.; Tan, K. L. *Chem. Phys. Lett.* **2000**, *330*, 41–47.
- (7) Merkulov, V. I.; Guillorn, M. A.; Lowndes, D. H.; Simpson, M. L.; Voelkl, E. *Appl. Phys. Lett.* **2001**, *79*, 1178–1180.
- (8) Rider, A. E.; Levchenko, I.; Chan, K. K. F.; Tam, E.; Ostrikov, K. *J. Nanopart. Res.* **2008**, *10*, 249–254.
- (9) Melechko, A. V.; Merkulov, V. I.; McKnight, T. E.; Guillorn, M. A.; Klein, K. L.; Lowndes, D. H.; Simpson, M. L. *J. Appl. Phys.* **2005**, *97*, 041301.
- (10) Guillorn, M. A.; Yang, X.; Melechko, A. V.; Hensley, D. K.; Hale, M. D.; Merkulov, V. I.; Simpson, M. L.; Baylor, L. R.; Gardner, W. L.; Lowndes, D. H. *J. Vac. Sci. Technol., B* **2004**, *22*, 35–39.
- (11) Ye, Q.; Cassell, A.; Liu, H.; Chao, K.-J.; Han, J.; Meyyappan, M. *Nano Lett.* **2004**, *4*, 1301–1305.
- (12) Liu, J. W.; Kuo, Y. T.; Klabunde, K. J.; Rochford, C.; Wu, J.; Li, J. *ACS Appl. Mater. Interfaces* **2009**, *1*, 1645–1649.
- (13) Guillorn, M. A.; McKnight, T. E.; Melechko, A.; Merkulov, V. I.; Britt, P. F.; Austin, D. W.; Lowndes, D. H.; Simpson, M. L. *J. Appl. Phys.* **2002**, *91*, 3824–3828.
- (14) Fletcher, B. L.; Hullander, E. D.; Melechko, A. V.; McKnight, T. E.; Klein, K. L.; Hensley, D. K.; Morrell, J. L.; Simpson, M. L.; Doktycz, M. J. *Nano Lett.* **2004**, *4*, 1809–1814.
- (15) Hyeon, T.; Lee, S. S.; Park, J.; Chung, Y.; Bin Na, H. *J. Am. Chem. Soc.* **2001**, *123*, 12798–12801.
- (16) Sun, S. H.; Zeng, H.; Robinson, D. B.; Raoux, S.; Rice, P. M.; Wang, S. X.; Li, G. X. *J. Am. Chem. Soc.* **2004**, *126*, 273–279.
- (17) Teng, X. W.; Yang, H. *J. Mater. Chem.* **2004**, *14*, 774–779.
- (18) Woo, K.; Hong, J.; Choi, S.; Lee, H. W.; Ahn, J. P.; Kim, C. S.; Lee, S. W. *Chem. Mater.* **2004**, *16*, 2814–2818.
- (19) Redl, F. X.; Black, C. T.; Papaefthymiou, G. C.; Sandstrom, R. L.; Yin, M.; Zeng, H.; Murray, C. B.; O'Brien, S. P. *J. Am. Chem. Soc.* **2004**, *126*, 14583–14599.
- (20) Park, J.; Lee, E.; Hwang, N. M.; Kang, M. S.; Kim, S. C.; Hwang, Y.; Park, J. G.; Noh, H. J.; Kini, J. Y.; Park, J. H.; et al. *Angew. Chem., Int. Ed.* **2005**, *44*, 2872–2877.
- (21) Sun, S. H.; Murray, C. B. *J. Appl. Phys.* **1999**, *85*, 4325–4330.
- (22) Puentes, V. F.; Zanchet, D.; Erdonmez, C. K.; Alivisatos, A. P. *J. Am. Chem. Soc.* **2002**, *124*, 12874–12880.
- (23) Tracy, J. B.; Weiss, D. N.; Dinega, D. P.; Bawendi, M. G. *Phys. Rev. B* **2005**, *72*, 064404.
- (24) Bao, Y.; An, W.; Turner, C. H.; Krishnan, K. M. *Langmuir* **2010**, *26*, 478–483.
- (25) Park, J.; Kang, E.; Son, S. U.; Park, H. M.; Lee, M. K.; Kim, J.; Kim, K. W.; Noh, H. J.; Park, J. H.; Bae, C. J.; et al. *Adv. Mater.* **2005**, *17*, 429–434.
- (26) Lee, I. S.; Lee, N.; Park, J.; Kim, B. H.; Yi, Y. W.; Kim, T.; Kim, T. K.; Lee, I. H.; Paik, S. R.; Hyeon, T. *J. Am. Chem. Soc.* **2006**, *128*, 10658–10659.
- (27) Winnischofer, H.; Rocha, T. C. R.; Nunes, W. C.; Socolovsky, L. M.; Knobel, M.; Zanchet, D. *ACS Nano* **2008**, *2*, 1313–1319.
- (28) Johnston-Peck, A. C.; Wang, J. W.; Tracy, J. B. *ACS Nano* **2009**, *3*, 1077–1084.
- (29) Wang, J. W.; Johnston-Peck, A. C.; Tracy, J. B. *Chem. Mater.* **2009**, *21*, 4462–4467.
- (30) Park, J.; Joo, J.; Kwon, S. G.; Jang, Y.; Hyeon, T. *Angew. Chem., Int. Ed.* **2007**, *46*, 4630–4660.
- (31) Kim, J.; Rong, C. B.; Lee, Y.; Liu, J. P.; Sun, S. H. *Chem. Mater.* **2008**, *20*, 7242–7245.
- (32) Seo, W. S.; Lee, J. H.; Sun, X. M.; Suzuki, Y.; Mann, D.; Liu, Z.; Terashima, M.; Yang, P. C.; McConnell, M. V.; Nishimura, D. G.; et al. *Nat. Mater.* **2006**, *5*, 971–976.
- (33) Desvoux, C.; Amiens, C.; Fejes, P.; Renaud, P.; Respaud, M.; Lecante, P.; Snoeck, E.; Chaudret, B. *Nat. Mater.* **2005**, *4*, 750–753.

- (34) Merkulov, V. I.; Lowndes, D. H.; Wei, Y. Y.; Eres, G.; Voelkl, E. *Appl. Phys. Lett.* **2000**, *76*, 3555–3557.
- (35) Cui, H. T.; Yang, X. J.; Simpson, M. L.; Lowndes, D. H.; Varela, M. *Appl. Phys. Lett.* **2004**, *84*, 4077–4079.
- (36) Denysenko, I.; Ostrikov, K. J. *Phys. D: Appl. Phys.* **2009**, *42*, 015208.
- (37) Railsback, J. G.; Johnston-Peck, A. C.; Wang, J. W.; Tracy, J. B. *ACS Nano* **2010**, *4*, 1913–1920.
- (38) Liu, S. H.; Gao, H. T.; Ye, E. Y.; Low, M.; Lim, S. H.; Zhang, S. Y.; Lieu, X. H.; Tripathy, S.; Tremel, W.; Han, M. Y. *Chem. Commun.* **2010**, *46*, 4749–4751.
- (39) Lu, A. H.; Li, W. C.; Matoussevitch, N.; Spliethoff, B.; Bönnemann, H.; Schüth, F. *Chem. Commun.* **2005**, 98–100.
- (40) Helveg, S.; López-Cartes, C.; Sehested, J.; Hansen, P. L.; Clausen, B. S.; Rostrup-Nielsen, J. R.; Abild-Pedersen, F.; Nørskov, J. K. *Nature* **2004**, *427*, 426–429.
- (41) Ichihashi, T.; Fujita, J.; Ishida, M.; Ochiai, Y. *Phys. Rev. Lett.* **2004**, *92*, 215702.
- (42) Ichihashi, T.; Ishida, M.; Ochiai, Y.; Fujita, J. *J. Vac. Sci. Technol., B* **2004**, *22*, 3221–3223.
- (43) Yang, X. J.; Guillorn, M. A.; Austin, D.; Melechko, A. V.; Cui, H. T.; Meyer, H. M.; Merkulov, V. I.; Caughman, J. B. O.; Lowndes, D. H.; Simpson, M. L. *Nano Lett.* **2003**, *3*, 1751–1755.
- (44) Clearfield, R.; Railsback, J. G.; Pearce, R. C.; Hensley, D. K.; Fowlkes, J. D.; Fuentes-Cabrera, M.; Simpson, M. L.; Rack, P. D.; Melechko, A. V. *Appl. Phys. Lett.* **2010**, *97*, 253101.
- (45) Cai, D.; Doughty, C. A.; Potocky, T. B.; Dufort, F. J.; Huang, Z.; Blair, D.; Kempa, K.; Ren, Z. F.; Chiles, T. C. *Nanotechnology* **2007**, *18*, 365101.
- (46) Chhowalla, M.; Teo, K. B. K.; Ducati, C.; Rupesinghe, N. L.; Amaratunga, G. A. J.; Ferrari, A. C.; Roy, D.; Robertson, J.; Milne, W. I. *J. Appl. Phys.* **2001**, *90*, 5308–5317.
- (47) Identification of certain commercial equipment, instruments, or materials in this paper does not imply recommendation or endorsement by the National Institute of Standards and Technology, nor does it imply that the products are necessarily the best available for the purpose.
- (48) Aliaga, C.; Park, J. Y.; Yamada, Y.; Lee, H. S.; Tsung, C. K.; Yang, P. D.; Somorjai, G. A. *J. Phys. Chem. C* **2009**, *113*, 6150–6155.